Prediction of local scour depth at bridge piers under clear-water and live-bed conditions: comparison of literature formulae and artificial neural networks

E. Toth and L. Brandimarte

ABSTRACT

The scouring effect of the flowing water around bridge piers may undermine the stability of the structure, leading to extremely high direct and indirect costs and, in extreme cases, the loss of human lives. The use of Artificial Neural Network (ANN) models has been recently proposed in the literature for estimating the maximum scour depth around bridge piers: this study aims at further investigating the potentiality of the ANN approach and, in particular, at analysing the influence of the experimental setting (laboratory or field data) and of the sediment transport mode (*clear water* or *live bed*) on the prediction performances. A large database of both field and laboratory observations has been collected from the literature for predicting the maximum local scour depth as a function of a parsimonious set of variables characterizing the flow, the sediments and the pier. Neural networks with an increasing degree of specialization have been implemented – using different subsets of the calibration data in the training phase – and validated over an external validation dataset. The results confirm that the ANN scour depths' predictions outperform the estimates obtained by empirical formulae conventionally used in the literature and in the current engineering practice, and demonstrate the importance of taking into account the differences in the type of available data – laboratory or field data – and the sediment transport mode – clear water or live bed conditions.

Key words | bridge piers, empirical formulae, multi-layer feedforward networks, scour depth, sediment transport mode

E. Toth (corresponding author)
DICAM,
University of Bologna,
Italy,
Via Risorgimento 2,
Bologna,
Italy
E-mail: *elena.toth@unibo.it*

L. Brandimarte
UNESCO-IHE,
Institute for Water Education,
The Netherlands,
Westvest,
7, Delft,
The Netherlands

NOTATION

θ	angle of attack of the flow	g	gravitational acceleration
ϕ	Shields parameter	K_θ	angle of flow attack factor
ρ	water mass density	K_d	sediment size factor
v	cinematic viscosity of the fluid	K_I	flow intensity factor
ϕ_{sF}	Froelich pier shape factor	K_s	Melville pier shape factor
b	pier width	K_t	factor for the sediment mode transport
b_p	projected pier width	K_{yb}	depth size factor
d_{50}	median grain size	L	pier length
d_s	scour depth	V	mean flow velocity at the approach section
Fr	Froude number		
Fr_c	critical Froude number	V_c	critical velocity for sediment motion
N_s	Neill pier shape factor	y	approach flow depth

INTRODUCTION

The presence of a bridge structure in a flow channel inevitably involves a significant change to the flow pattern, which in turns induces the formation of a scour hole at the piers. The scouring effect of the flowing water around bridge piers is a common issue that engineers have to face both at the design and maintenance stages since it has been widely recognized (Federal Highway Administration 1988; Parola et al. 1997; Melville & Coleman 2000) as one of the main causes of bridge damage and failure, thus leading to extremely high direct and indirect costs and, in extreme cases, the loss of human lives.

The phenomenon is extremely complex: to the general erosion, causing a bed lowering, may be added the scour due to the flow contraction and the localized scour due to the formation of a system of vortices that develops around the pier when unidirectional flow in erodible channels becomes three-dimensional (Shen et al. 1969; Graf 1998; Melville & Coleman 2000).

Over the past decades the scientific community has made several efforts to investigate, with different approaches, the scour phenomenon around bridge piers, but relevant uncertainties still affect the prediction of the scour depth. Among the main reasons for such uncertainties we may cite (Franzetti et al. 1994; Federico et al. 2003) the difference between the actual geometrical description of piers and streambed and those schematized in the models, the time-dependent flow pattern and the scanty information often available for characterizing the sediments.

The most promising research approaches for studying the scour process are certainly those that model the temporal evolution of the scour hole (Franzetti et al. 1989; Kothyari et al. 1992; Briaud et al. 1999; Oliveto & Hager 2002; Mia & Nago 2003; Brandimarte et al. 2006) and, for real-world applications, the effect of variable streamflow should be taken into account: in fact, the time needed to get to an equilibrium scour depth may be extremely long in comparison with the short duration of the scour-generating flood events (characterized by high flow depths and velocities), thus leading to the risk of overestimating the actual erosion in unsteady flow conditions.

In order to fully describe such a complex physical phenomenon, detailed information on the flow, on the sediments, on the streambed and on the structure would be needed: such information is rarely available in real-world applications and it follows that, although scour formation is a time-dependent process, in current engineering practice, the scour depth is traditionally estimated by applying empirical formulae that do not take into account the time progression of the scour hole but try to identify only the anticipated maximum scour.

These equations were derived, over the past 50 years, by different authors interpreting the results of sets of experiments mainly carried out in laboratory settings. Many of them (but not all) take explicitly into account the nature of the sediment mode transport, which is one of the driving factors in the attainment of the equilibrium scour depth. In the *clear-water* mode, when the upstream bed material is not in motion, the scour depth increases slowly tending to a stable solution; in *live-bed* conditions, when there is transport of bed material from upstream, the scour depth increases rapidly and, due to the interaction between erosion and deposition, it tends to fluctuate around an equilibrium value (Melville & Chiew 1999; Oliveto & Hager 2002).

As an alternative to literature equations, in recent years, the application of Artificial Neural Networks (ANNs) to the estimate of local scour at bridge piers has been proposed (Jeng et al. 2005; Bateni et al. 2007a, b; Lee et al. 2007; Firat & Gungor 2009; Muzzammil & Ayyub 2010), taking advantage of their capability to flexibly reproduce the highly non-linear nature of the relationship between input and output variables, also when such relationship is not explicitly known a priori. However, many of these studies use limited datasets, either collected from laboratory experiments or from field measures and do not distinguish between scour occurring in the different conditions of *clear-water* (no sediment being transported into the scour hole by the flowing water) and *live-bed* (sediments are supplied at the pier site from upstream).

This paper presents the application of ANN models for the prediction of scour depth at bridge piers, taking explicitly into account the transport mode conditions, and in a rigorous calibration–validation framework. Observed scour records collected from different sources, and relative to both laboratory experiments and field campaigns, were used to create different training subsets, with an increasing degree of specialization: models distinguishing field and laboratory data, *clear-water* and *live-bed* conditions were applied to investigate the capability to predict the equilibrium

(or quasi-equilibrium) scour depth over an external validation data set. The performances obtained through the implementation of the ANNs are compared to those obtained by applying eight of the most widely used literature formulae to the same external validation data.

DATA SETS

Two large datasets were collected from the literature to carry out this investigation, including both in situ field scour measurements and data derived from laboratory experiments. Collecting both types of data is deemed to be useful both for increasing the data base and for analysing the performances attainable with the proposed methods when applied to different experimental settings. In fact, laboratory data are more accurate measurements but generally not representative of the actual conditions of real-world cases, that are often much more complex than those schematized by the laboratory equipment. On the other hand, field data describe real-world situations but are affected by significant uncertainties in the measurements of both input and output variables. Such uncertainties are due to the unavoidable simplification of the description of the real flow pattern, sediments' properties, pier and streambed geometry and are worsened by the absence of a standardized and objective data collection procedure.

The Field dataset includes observations collected by (i) Froelich (1988), reporting data relative to bridges located mainly in the USA but also in New Zealand and Serbia, and (ii) the U.S. Geological Survey (USGS) in cooperation with the Federal Highway Administration and other U.S. highway administrations (Mueller & Wagner 2005). The USGS national bridge scour database is formed of more than five hundred records, but including often more measurements relative to the same pier, and also some scour depths occurring downstream of the bridge: in such cases, for each pier, only the maximum upstream scour depth was selected in the present study. In addition, we discarded the measurements relative to groups of piers (more bridges in series), the scour values reported as influenced by floating debris accumulation and those with an incomplete description of pier geometry (length, in particular, was not always recorded).

The Laboratory dataset includes scour observations from laboratory experiments carried out by a number of scientists over the past decades, reporting the equilibrium (or quasi-equilibrium) scour depths obtained for a variety of experimental conditions. Many data were obtained by Kothyari (1989), which described also some results of *clear-water* experiments developed by Ettema (1980) and by Chabert & Engeldinger (1956); other records belonging to different experiments carried out by Ettema (1980) and by Chabert & Engeldinger (1956), along with three records of Chee (1982), were reported in Jeng *et al.* (2005). The other experiments are those described in Chiew (1984), Dey *et al.* (1995), Melville & Chiew (1999), Mia & Nago (2003), Sheppard *et al.* (2004), Sheppard & Miller (2006).

In addition to the scour depth measurement (or the estimate of the equilibrium or quasi-equilibrium depth), d_s, the following information was collected for all the piers of both field and laboratory data bases: mean velocity (V) and water depth (y) of the approach flow; mean particle diameter (d_{50}); dimension of the pier (width, b, and length, L); shape of the pier; angle of attack of the flow (θ).

In the absence of more detailed information on the incipient motion conditions, the distinction between *clear-water* or *live-bed* condition was performed by assuming *clear-water* conditions if the approach velocity V is less than the critical velocity for sediment motion, V_c, where this latter is estimated through Neill formula (Neill 1973) for the d_{50} size particles:

$$V_c = \phi^{0.5} 31.08 y^{1/6} d_{50}^{1/3}. \tag{1}$$

The Shields parameter, ϕ, in Equation (1) is computed with Equation (2), originally proposed by Miller *et al.* (1977) to relate the grain size to the shear velocity and then modified by Mueller (1996) for estimating the Shields parameter:

$$\begin{cases} \phi = 0.0019 d_{50}^{-0.384} & d_{50} < 0.0009m \\ \phi = 0.0942 d_{50}^{0.175} & \text{if} \quad 0.0009m < d_{50} < 0.020m \\ \phi = 0.047 & d_{50} > 0.020m. \end{cases} \tag{2}$$

The critical velocity was computed for all the records and the cases in which the V/V_c ratio resulted in too small a value (less than 0.35) were discarded since it was assumed that no scour is generated in such conditions.

The laboratory data were then carefully inspected in order to exclude the records in which the scour depth was obtained in *clear-water* experimental settings (that is where no sediments were supplied at the pier site by the flowing water) but with flow velocities higher than the critical ones (estimated with Equation (1)). Such experiments are in fact not representative of real-world applications, in which such high velocity would determine a *live-bed* condition.

The finally selected data base is formed by 215 (147 *live-bed* and 68 *clear-water*) field records and 331 (157 *live-bed* and 174 *clear-water*) laboratory records. All the eventually selected laboratory records correspond to cylindrical piers: it follows that all the pier noses are circular, the flow attack angle is null and the pier length is equal to its width for all the laboratory data.

The four sets (dividing field from laboratory data and *clear-water* from *live-bed* conditions) were then divided into calibration data (2/3 of the total), used for ANN training, and validation data (the remaining 1/3 of the records), for the fair evaluation of both ANN and literature formulae.

The ranges of the measured variables characterizing the selected records are summarized in Table 1.

ESTIMATION OF LOCAL SCOUR WITH ARTIFICIAL NEURAL NETWORKS

As an alternative to the traditional literature formulae, ANNs are implemented as non-linear models for identifying the relationship between the flow, sediment and pier characteristics and the equilibrium scour depth.

ANNs have been widely applied in the last decade to a variety of hydrologic and hydraulic problems (see among many others, Abrahart *et al.* 1999; Giustolisi 2000; Liriano & Day 2001; Bowden *et al.* 2003; Rao & Alvarruiz 2007; Tsanis *et al.* 2008; Toth 2009) mainly due to their capability to flexibly reproduce highly non-linear relationships; the method is a data-driven approach, where no a priori relationship between known parameters and observed values has to be hypothesized and no knowledge of the underlying process is needed.

The ANN models implemented in the present work (using MATLABs Neural Network Toolbox) are multi-layer feedforward networks formed by only one hidden layer; a tan-sigmoidal activation function was chosen for the hidden layer and a linear transfer function for the output layer. The training algorithm, minimizing a learning function expressing the closeness between observations and ANN outputs, in the present case the mean squared error, is the Newton Levenberg–Marquardt BackPropagation algorithm (Hagan & Menhaj 1994), that approaches second-order training speed without having to compute the Hessian matrix. The algorithm was designed to serve as an intermediate optimization algorithm between the Gauss–Newton method and the gradient descent algorithm, and addresses the limitations of each of those techniques. The control parameter that governs the relative influence of the two techniques starts from a value of 0.001, is decreased after each successful step (reduction in error function) and is increased when a tentative step would increase the error function: the decreasing and increasing factors are respectively 0.1 and 10. To mitigate overfitting and to improve generalization, a Bayesian regularization of the

Table 1 │ Range of observed variables for the selected datasets

Variable	Field data Live bed	Field data Clear water	Laboratory data Live bed	Laboratory data Clear water
d_{50} (mm)	0.01–33	0.06–108	0.2–5.35	0.22–3
y (m)	0.27–22.52	0.3–9.17	0.05–0.43	0.02–1.9
V (m)	0.46–4.08	0.18–3.51	0.32–2.16	0.17–0.76
b (m)	0.29–19.50	0.3–4.60	0.03–0.15	0.02–0.91
L (m)	0.98–39	3.41–27.43	0.03–0.15	0.02–0.91
θ (°)	0–43	0–85	0	0
Pier nose shape	square- circ-triang	square- circ-triang	circular	circular
d_s (m)	0.15–10.40	0.15–2.44	0.03–0.3	0–1.39

learning function (Foresee & Hagan 1997) was applied. In order to prevent the training algorithm from being trapped in a local minimum, each ANN is trained (for 50 epochs) starting from 10 different initial networks, randomly initialized, of which the best performing on training data (without making any use of validation data) is chosen as the trained network.

Input variables

The input nodes to be included in a neural network may be decided on the basis of a priori considerations (for example as a function of the physics of the analysed phenomenon) or analysing the influence of a wide set of possible input variables on the target. This last approach may be carried out either with a model-free methodology, using statistical measures of dependence (such as correlation or mutual information) to determine the strength of the relationship between candidate model inputs and the model output, prior to model specification and calibration (e.g., Solomatine & Dulal 2003; Bowden et al. 2005; Lin et al. 2006; Wang et al. 2009), or with a model-based approach, that analyses the performance of calibrated models with different inputs for choosing the most appropriate input vector.

In the present work, the input variables were decided a priori, consisting in the characteristics (among those that are actually available in all the collected datasets) of flow, sediments and structure that are considered as the most influential on the basis of the physics of the scour phenomenon and consistently with the scientific literature (e.g. Ettema et al. 1998; Choi & Cheong 2006; Bateni et al. 2007a). This allows also a fair comparison of the ANN models with the empirical formulae that are world-widely applied both in the literature and in the operational engineering practice.

The input nodes feed to the network the variables that were actually measured for each data record (that is, for each pier): mean velocity (V) and water depth (y); mean particle diameter (d_{50}); dimension of the pier (width, b, and length, L); shape of the pier; angle of attack of the flow (θ).

As far as the shape of the pier nose is concerned, such information is made quantitative through the widely-used Neill shape coefficient (Neill 1973), here denoted by N_s: 1 for square pier noses, 2 for circular noses, 3 for sharp noses.

The "indirect" variables (for example Froude number or critical velocity) that are often used in the literature formulae but are derived as functions of "direct" variables that were actually measured, were not included as input. Also the variables that are assumed to be constant, in the usual conditions of laboratory and field experiments, for all the records (i.e. flow density, flow viscosity, acceleration due to gravity) are not used as input variables. In fact, adding input data that do not actually convey any new information to the model would only increase, along with the number of input nodes, the number of parameters to be calibrated, therefore leading to a risk of overfitting in the training phase. It was chosen to not non-dimensionalize (nor to combine the data in other ways) such attributes (for example making the ratio of scour depth with pier width or with flow depth), in order not to lose information on the direct relationship of each of them with the output (that is, the scour depth). Such choice is supported by the results obtained, in a similar application based on laboratory data only, by Bateni et al. (2007b), where the "predictions based on the original (dimensional) scour data were better than those based on dimensionless forms of the data."

The only exception to this rule is the combination of pier length (L) and angle of attack of the flow (θ), since their influence is strictly related (actually, the pier length has no influence on the upstream scour when the attack angle is zero): in order to decrease the number of input variables, and therefore of parameters to be calibrated, these two attributes are presented to the network in the form of the K_θ parameter used both in the Colorado State University (Richardson & Davis 1995) and in the Melville & Chiew (1999) equations:

$$K_\theta = \left[\frac{L}{b}\sin(\theta) + \cos(\theta)\right]^{0.65}. \tag{3}$$

Both input attributes and the output have been standardized to have, for each input variable, mean equal to zero and variance equal to one. In fact, standardizing input and target variables tends to make the training process better behaved by improving the numerical condition of the optimization problem and ensuring that the default values involved in initialization and termination are appropriate (see Sarle 1997), so as to make training faster and to reduce the chances of getting stuck in local minima.

The input variables provided to the ANN are therefore the following: (i) pier width (b), (ii) mean approach flow velocity (V), (iii) approach water depth (y), (iv) mean sediment diameter (d_{50}), (v) Neill shape coefficient (N_s), (vi) Melville angle of attack coefficient (K_θ).

ANN models

Due to the different nature of the measuring conditions in laboratory and field experiments and in order to verify the influence of the sediment transport mode (*clear-water* or *live-bed*), different ANN models are implemented for predicting the scour depth over the four validation data sets: (a) field *clear-water* (Val F-CW); (b) field *live-bed* (Val F-LB); (c) laboratory *clear-water* (Val L-CW); (d) laboratory *live-bed* (Val L-LB).

Seven neural networks have been implemented, using seven different subsets of the calibration data in the training phase, with an increasing specialization degree. The first model was parametrized using all the data available in the training set (two thirds of all the available data, since the remaining third is dedicated to validation), both field and laboratory, *clear-water* or *live-bed*, for a total of 315 records. Such model, denoted *Model FL* model is a "universal" model and it was applied for the prediction of all the four validation subsets.

Laboratory and field training data were then separated, obtaining *Model F*, to be used for predicting the scours of Val F-CW and Val F-LB, and *Model L*, to be used for predicting the scours of Val L-CW and Val L-LB.

Finally, the most specialized models are implemented, distinguishing both experimental setting and sediment transport mode, training four models: *Model F-CW*, *Model F-LB*, *Model L-CW* and *Model L-LB*, to be used exclusively on the validation data of the same type.

It must be noted that when dealing with laboratory data alone, that is for models *L*, *L-CW* and *L-LB*, the Neill shape coefficient (N_s) and the Melville angle of attack coefficient (K_θ) are not provided in input to the networks. In fact they have all the same value for the cylindrical piers of the laboratory experiments and their inclusion would increase the model complexity without adding any new information content. It follows that the input layer is, for such models, formed by four instead of six nodes.

The optimal number of hidden nodes to be included in the network is strongly case-dependent. In the present work, a trial-and-error procedure based on a "forward selection method" was implemented, beginning by selecting a small number of neurons and then increasing it. The hidden layer dimension providing the best trade-off between parsimony and forecasting performances, for each different model, as described below, was identified and is reported, for each ANN model, in Table 2.

The goodness-of-fit of the proposed models is evaluated through the mean absolute error (MAE), between the N_{val} records of observed, $d_{s,o}$, and predicted, $d_{s,p}$, scour depths,

$$MAE = \frac{\sum_{i=1}^{N_{val}} |d_{s,o}(i) - d_{s,p}(i)|}{N_{val}} \tag{4}$$

and by scatterplots of predicted versus observed scour depths, obtained with the different models (with increasing specialization) over the validations subsets. Only the results of the best-performing architecture (for each model type) are shown in Table 2 and Figure 1.

Table 2 | Mean absolute error, MAE (m), of the ANN models, over the different validation data types and number of hidden nodes (NH) in the selected architecture

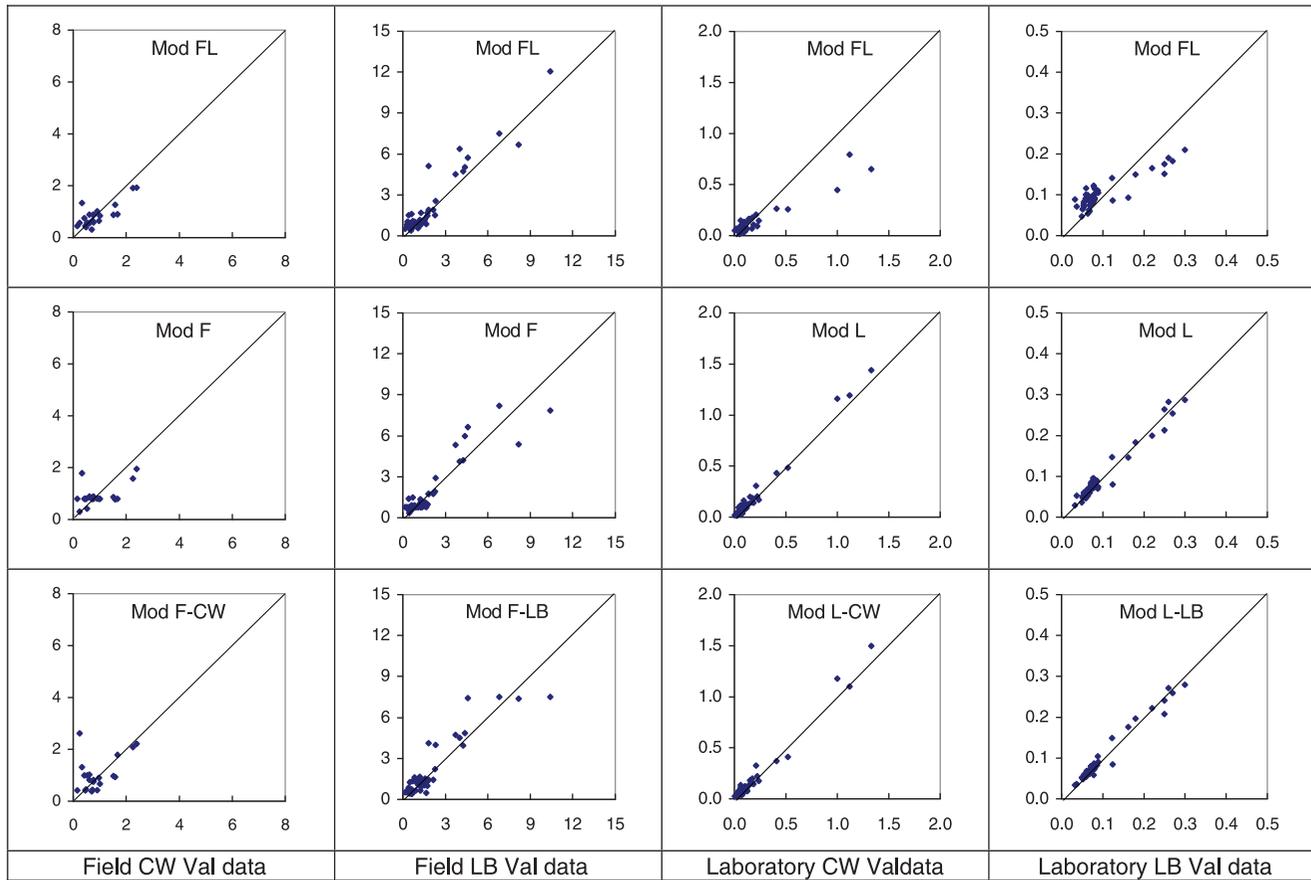| Validation set | ANN models (data type used in calibration) and number of hidden nodes (HN) | | | | | | |
	FL model (3 NH)	F model (3 NH)	F-CW model (3 NH)	F-LB model (3 NH)	L model (5 NH)	L-CW model (4 NH)	L-LB model (6 NH)
F	0.45	0.48					
F-CW	0.29	0.37	0.39				
F-LB	0.52	0.53		0.52			
L	0.05				0.02		
L-CW	0.064				0.026	0.020	
L-LB	0.029				0.009		0.006

Figure 1 | Scatterplot of predicted (*y*-axis) versus observed (*x*-axis) scour depths (*m*), obtained over the validations subsets with the ANN different models (from the general one to the more specialized).

Discussion of the ANN results

A clearly different behaviour of the laboratory and field data is highlighted, when considering the performances obtained with ANN models going from the more general (*FL model*, including all kind of data in calibration) to the more specialized ones (*F-CW, F-LB, L-CW, L-LB models*), passing through the intermediate ones (*F model* and *L model*).

In fact on the laboratory data there is a strong improvement of the performance when using the more specialized models: especially important is the enhancement going from the universal model (*FL*) to the one using only laboratory data (*L model*), but further improvement, even if to a lesser extent, is allowed by the even more specifically tailored models, trained exclusively on the same kind of sediment

supply conditions (*L-CW* and *L-LB*) that are considered in validation.

On the contrary, the estimation of field data does not improve with the more specialized models but it is always better with the general model (*FL model*), deteriorating for increasing specialization.

The reason for this behavior may be sought in the quality of the data: laboratory measurements are high-quality data, accurate and actually representative of the study case (that is of course much less complex than real-world cases). Such high-quality information content may be fully exploited by the more specialized models, even when trained on relatively small numbers of observations as those characterizing these models. In fact, data of such good quality are not affected by significant noise and are therefore less subject to overfitting.

On the other hand, field data are much less accurate and representative, given the meagre information we have on the measurement procedures and in particular on the characterization of the approach flow (especially because of the unsteady state conditions) and of upstream sediment properties and behaviour. When training a model on a small set of noisy data, affected by relevant uncertainty, the risk of overfitting, when model parameters fit also the noise of the training data, is very high. In the present study, this is shown by the poor performance over external validation data that are obtained by the models based on calibration sets formed by field data only. The generalization capacity, and therefore the performances over external field data, improves when adding the high-quality laboratory data to the training set (model FL), since the merged training data set is both larger and less noisy.

ESTIMATION OF LOCAL SCOUR WITH EMPIRICAL FORMULAE

Scientific literature has provided, over the past decades, a number of experimental equations for estimation of the maximum depth of local scour at bridge piers. In the present study, eight of the most widely used empirical equations (reported in Table 3) were used as a term of comparison for evaluating the performances of the ANN models.

The majority of such formulae have been developed aiming at interpolating the envelope curve of data recorded in laboratory experiments, with the exception of Froelich's equation (1988), which was obtained for interpolating field measurements and in particular under *live-bed* sediment transport conditions.

Table 3 | Empirical formulae used for estimating pier scour depth (meaning of the symbols is reported in the text)

1)	Laursen & Toch (1956)	$d_s = 1.35 * b^{0.7} * y^{0.3}$
2)	Shen et al. (1969)	$d_s = 0.00023 * \left(\dfrac{Vb}{v}\right)^{0.619}$
3)	Hancu (1971)	$d_s = 2.42b * \left(2\dfrac{V}{V_c} - 1\right) * \left(\dfrac{V_c^2}{gb}\right)^{1/3}$
4)	Breusers et al. (1977)	$d_s = b * \left(\dfrac{2V}{V_c} - 1\right) * [2\tanh(y/b)] * K_s * K_\theta$ for $0.5 < V/V_c < 1$ $d_s = b * [2\tanh(y/b)] * K_s * K_\theta$ for $V/V_c > 1$
5)	Jain & Fischer (1980)	$d_{sa} = 2.0 * b * (Fr - Fr_c)^{0.25}(y/b)^{0.5}$ for $(Fr - Fr_c) > 0.2$ $d_{sb} = 1.85 * b * Fr^{0.25} * (y/b)^{0.5}$ for $(Fr - Fr_c) < 0$ $d_s = \max(d_{sa}, d_{sb})$ for $0 < (Fr - Fr_c) < 0.2$
6)	Froelich (1988)	$d_s = 0.32 * \phi_{s,F} * b_p^{0.62} * y^{0.47} * Fr^{0.22} * d_{50}^{-0.09}$
7)	CSU (Richardson & Davis 1995)	$d_s = 2 * b * K_s * K_\theta * K_t * (y/b)^{0.35} Fr^{0.43}$
8)	Melville & Chiew (1999)	$d_s = b * K_s * K_\theta * K_{yb} * K_I * K_d$

The eight empirical equations were applied over all the validation subsets and the corresponding mean absolute error (MAE) and scatterplots of estimated versus observed scour depths are presented in Table 4 and Figures 2 and 3.

The results obtained by the literature formulae show that the Froelich equation, originally derived for *live-bed* conditions from field data only, is able to predict reasonably well both the field datasets, under *clear-water* and *live-bed* conditions; on the other hand, as expectable, it strongly underestimates laboratory data, getting the worst performances in comparison to the other formulae, that are all derived specifically on the basis of laboratory experiments.

The Jain & Fischer, CSU, Laursen & Toch and Melville & Chiew equations definitely tend to overestimate field data (some points obtained with the latter two are not shown in the scatterplot being out of scale): this was predictable, since, as said in the introduction, in field, real-world conditions, the flow is unsteady and the recorded values of water depths and flow velocities are the highest ones, generally lasting for periods (flood events) that are too short for reaching equilibrium (or quasi-equilibrium).

Analysing the laboratory data, the best match between predicted and observed scour depth is given by the equations of Laursen & Toch, Jain & Fischer and CSU, for both *live-bed* and *clear-water* conditions. Hancu and especially Breusers *et al.* equations experience more difficulties in the reproduction of *clear-water* laboratory data. Shen formula, not distinguishing the transport condition mode, overestimates the laboratory *live-bed* records, while it tends to underestimate the *clear water* ones. The Melville & Chiew equation seems to be excessively conservative as far as *live-bed* laboratory data are concerned.

CONCLUSIONS

The prediction of the maximum expected scour depth at bridge piers is a crucial step in the safe design of a bridge crossing. In the common practice, empirical derived equations are still used for estimating the pier scour depth. The application of such formulae, often derived by regression analysis on laboratory data, to real cases often leads to inaccurate pier design.

The growing interest for soft computing techniques and data driven approaches has spurred researchers to investigate the potentialities of applying hydroinformatics techniques to assist the estimation of the maximum scour depth at bridge piers. Building on the progress recently made to improve the performance of the scour estimate through the application of ANNs, we found that a more accurate analysis should take into account the differences in the type of available data – laboratory or field data – and the sediment transport mode – clear-water or live-bed conditions.

Multi-layer feedforward networks were implemented on extensive datasets using seven different subsets of the calibration data in the training phase, distinguishing the type of data and the sediment transport mode.

The performances of the implemented ANN were then compared to those of eight empirical formulae commonly used in engineering practice. Both the scatterplots (Figures 1–3) and the values of the mean absolute errors (see Tables 2 and 4) demonstrate that the best performing ANN models always allow a closer fit of the scour depth estimates to the observed measurements, over all the validation sets and especially for laboratory data. The MAE obtained with the most specialized ANNs on laboratory

Table 4 | Mean absolute error, MAE (m), of the formulae of Table 3, over the different validation data types

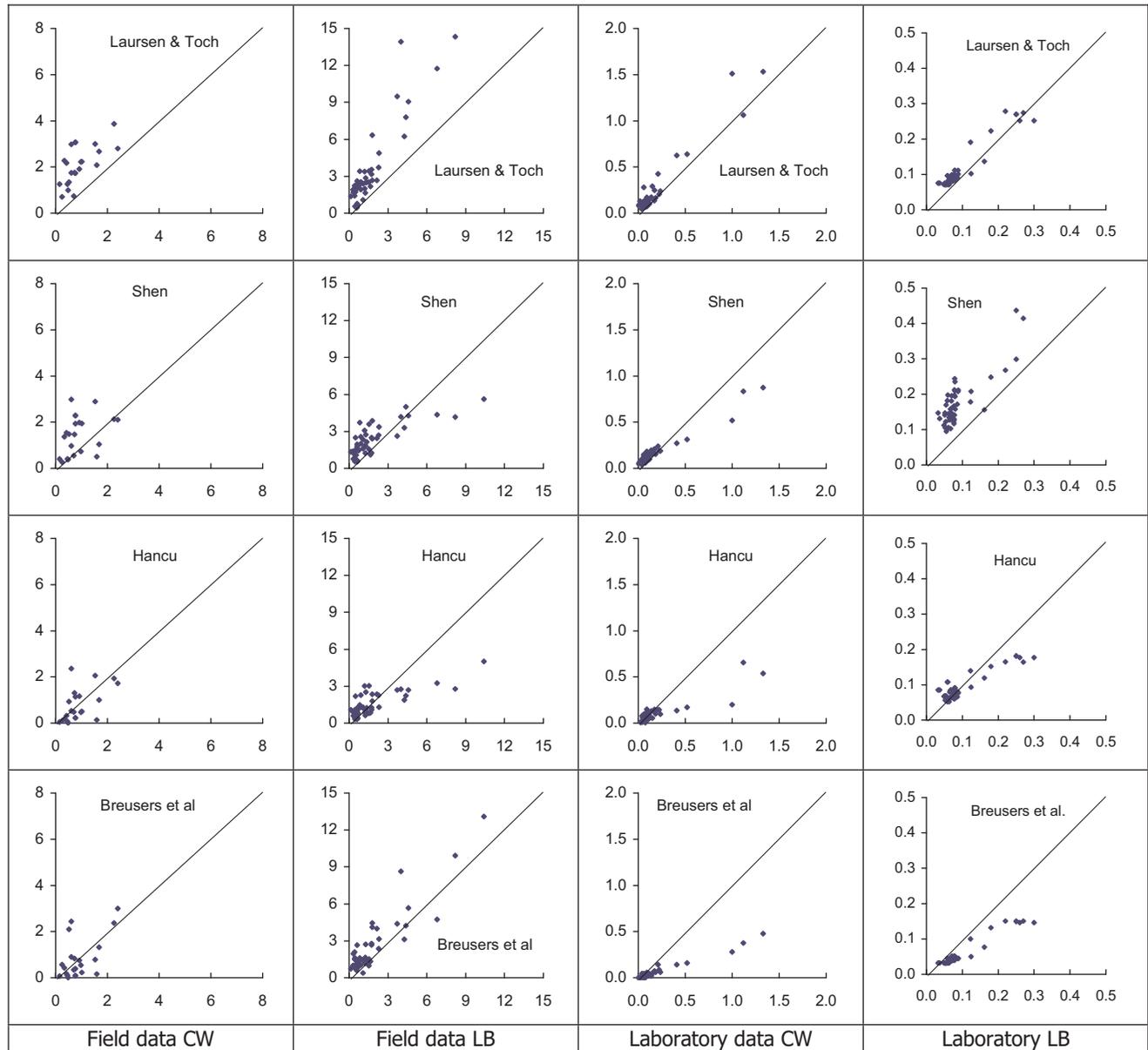| Validation set	Shen	Hancu	Laursen & Toch	Froelich	Jain & Fischer	Melville & Chiew	Breusers *et al*.	CSU
F	0.93	0.78	1.79	0.52	1.66	3.97	0.79	1.30
F-CW	0.78	0.49	1.18	0.46	1.22	2.32	0.55	1.18
F-LB	1.00	0.92	2.06	0.54	1.85	4.71	0.90	1.36
L	0.071	0.052	0.039	0.082	0.037	0.046	0.073	0.039
L-CW	0.051	0.077	0.053	0.098	0.050	0.050	0.102	0.051
L-LB	0.093	0.023	0.022	0.064	0.022	0.042	0.039	0.024

Figure 2 | Scatterplot of predicted (y-axis) versus observed field (x-axis) scour depths (m), obtained over the validations subsets by applying empirical formulae (1)–(4) of Table 3.

validation data is in fact less than one-half than that corresponding to the best-performing empirical formulae for the clear-water set and less than one-third for live-bed data.

The improvement offered by ANN models is less remarkable in the reproduction of field data, probably because of the high uncertainties and dishomogeneity of the measures and of the information, necessarily incomplete, describing the real-world cases and in particular the sediments' properties. The

difficulties experienced in the reproduction of the field data is probably the main limitation of the proposed approach, as of all the methodologies (notwithstanding the nature of the approach) proposed, so far, in the literature for the prediction of the maximum scour depth in real-world conditions.

Nonetheless, the presented approach based on neural networks, being able to exploit at the most the available
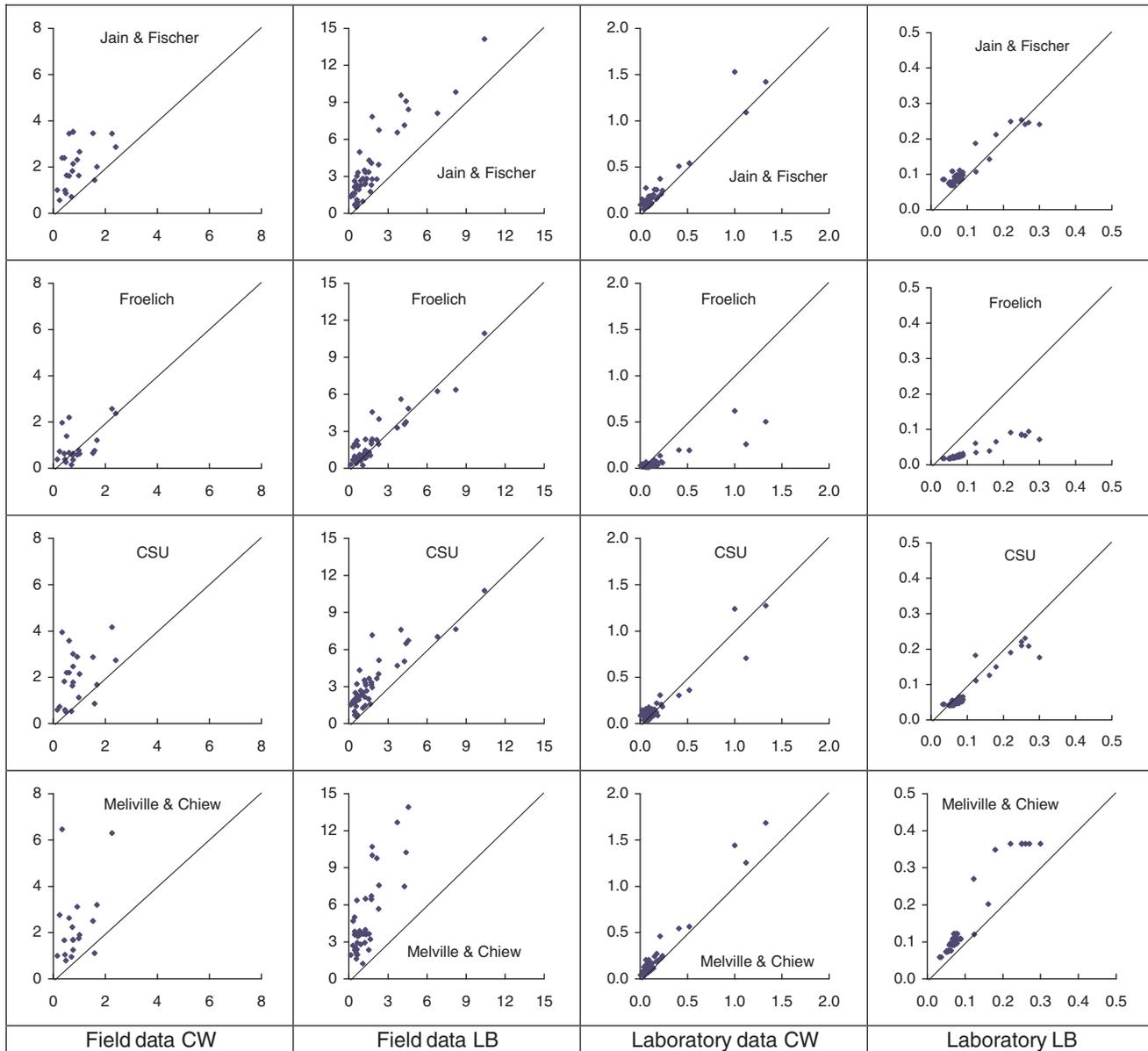
Figure 3 | Scatterplot of predicted (y-axis) versus observed field (x-axis) scour depths (m), obtained over the validations subsets by applying empirical formulae (5)–(8) of Table 3.

training data, may overall be considered an advantageous alternative to the traditional literature formulae typically used in engineering practice, under both clear-water and live-bed sediment transport conditions.

An additional limitation of the study is that the proposed method does not distinguish between underestimation and overestimation errors, whereas, in the engineering practice, at the design stage, it is undesirable to underpredict scour.

Future research work will focus in this direction, i.e. developing a neural network model able to restrain the underestimation of the scour depths.

anonymous referees for their constructive and helpful comments, which certainly enhanced the quality and readability of the paper.

REFERENCES

Abrahart, R. J., See, L. & Kneale, P. E. 1999 Using pruning algorithms and genetic algorithms to optimize network architectures and forecasting inputs in a neural network rainfall–runoff model. *J. Hydroinf.* **1**, 103–114.

Bateni, S. M., Borghei, S. M. & Jeng, D.-S. 2007a Neural network and neuro-fuzzy assessments for scour depth around bridge piers. *Engng Appl. Artif. Intell.* **20**(3), 401–414.

Bateni, S. M., Jeng, D.- S. & Melville, B. W. 2007b Bayesian neural networks for prediction of equilibrium and time-dependent scour depth around bridge piers. *Adv. Engng Softw.* **38**(2), 102–111.

Bowden, G. J., Dandy, G. C. & Maier, H. R. 2003 Data transformation for neural network models in water resources applications. *J. Hydroinf.* **5**, 245–258.

Bowden, G. J., Dandy G. C. & Maier, H. R. 2005 Input determination for neural network models in water resources applications. Part 1 – background and methodology. *J. Hydrol.* **301**, 75–92.

Brandimarte, L., Montanari, A., Briaud, J.-L. & D'Odorico, P. 2006 Stochastic flow analysis for predicting river scour of cohesive soils. *J. Hydraul. Engng* **132**(5), 493–500.

Breusers, H. N. C., Nicollet, G. & Shen, H. W. 1977 Local scour around cylindrical piers. *J. Hydraul. Res.* **15**(3), 211–52.

Briaud, J.-L., Ting, F. C. K., Chen, H. C., Guadavalli, R., Perugu, S. & Wei, G. 1999 SRICOS: prediction of scour rate in cohesive soils at bridge piers. *J. Geotech. Geoenviron. Engng* **125**(4), 237–246.

Chabert, J. & Engeldinger, P. 1956 *Etude des affouillements autour des piles des ponts*. Laboratoire d'Hydraulique, Chatou, France (in French).

Chee, R. K. W. 1982 Live-bed scour at bridge piers. *Report No. 290*. School of Engineering, University of Auckland, New Zealand.

Chiew, Y. M. 1984 Local scour at bridge piers. *Report No. 355*. Department of Civil Engineering, University of Auckland, New Zealand.

Choi S. & Cheong, S. 2006 Prediction of local scour around bridge piers using artificial neural networks. *J. Am. Water Resour. Assoc.* **42**, 487–494.

Dey, S., Bose, S. K. & Sastry, G. L. N. 1995 Clear-water scour at circular piers: a model. *J. Hydraul. Engng* **121**(12), 869–876.

Ettema, R. 1980 Scour at bridge piers. *Report No. 216*. School of Engineering, University of Auckland, New Zealand.

Ettema, R., Melville, B. W. & Barkdoll, B. 1998 Scale effect of pier-scour experiments. *J. Hydraul. Engng.* **124**(6), 639–642.

Federal Highway Administration 1988 *Revisions to the National Bridge Inspection Standards*. Technical Advisory T5140.21. FHA, McLean, VA.

Federico, F., Silvagni, G. & Volpi, F. 2003 Scour vulnerability of river bridge piers. *J. Geotech. Geoenviron. Engng* **129**(10), 890–899.

Firat, M. & Gungor, M. 2009 Generalized regression neural networks and feed forward neural networks for prediction of scour depth around bridge piers. *Adv. Engng Softw.* **40**(8), 731–737.

Foresee, F. D. & Hagan, M. T. 1997 Gauss–Newton approximation to Bayesian learning. *IEEE Int. Conf. on Neural Networks*, 3, New York, 1930–1935.

Franzetti, S., Larcan, E. & Mignosa, P. 1989 Erosione alla base di pile circolari di ponti: Verifica sperimentale dell'ipotesi di esistenza di una situazione finale di equilibrio. *Idrotecnica* **16**(3), 135–141 (in Italian).

Franzetti, S., Malavasi, S. & Piccinin, C. 1994 Sull'erosione alla base delle pile di ponte in acque chiare. *Atti XXIV Convegno di Idraulica e Costruzioni Idrauliche, Napoli*, **4**, 13–24 (in Italian).

Froelich, D. C. 1988 Analysis of onsite measurements of scour at piers. *ASCE Natl Conf. on Hydraulic Engineering*. ASCE, Colorado Springs, CO, pp. 534–539.

Giustolisi, O. 2000 Input–output dynamic neural networks simulating inflow–outflow phenomena in an urban hydrological basin. *J. Hydroinf.* **2**(4), 269–279.

Graf, W. H. 1998 *Fluvial Hydraulics*. Wiley, New York.

Hagan, M. T. & Menhaj, M. 1994 Training feedforward networks with the Marquardt algorithm. *IEEE Trans. Neural Netw.* **5**(6), 989–993.

Hancu, S. 1971 Sur le calcul des affouillements locaux dams la zone des piles des ponts. *Proc. 14th IAHR Congress*, Paris, France, Vol. 3, International Association for Hydraulic Research, Delft, The Netherlands, pp. 299–313.

Jain, S. C. & Fischer, E. E. 1980 Scour around bridge piers at high flow velocities. *J. Hydraul. Engng* **106**(11), 1827–1842.

Jeng, D.- S., Bateni, S. M. & Lockett, E. 2005 Neural Network assessment for scour depth around bridge piers. *Research Report No R855*, Department of Civil Engineering, University of Sydney.

Kothyari, U. C. 1989 Scour around bridge piers. *Ph.D. Thesis*, University of Roorkee, India.

Kothyari, U. C., Garde, R. J. & Ranga Raju, K. G. 1992 Temporal variation of scour around circular bridge piers. *J. Hydraul. Engng* **118**(8), 1091–1106.

Laursen, E. M. & Toch, A. 1956 *Scour around Bridge Piers and Abutments*. Bulletin No. 4. Iowa Highway Research Board, Ames, IA.

Lee, T. L., Jeng, D. S., Zhang, G. H. & Hong, J. H. 2007 Neural network modelling for estimation of scour depth around bridge piers. *J. Hydrodyn.* **19**(3), 378–386.

Lin, J. Y., Cheng, C. T. & Chau, K. W. 2006 Using support vector machines for long-term discharge prediction. *Hydrol. Sci. J.* **51**, 599–612.

Liriano, S. L. & Day, R. A. 2001 Prediction of scour depth at culvert outlets using neural networks. *J. Hydroinf.* **3**(4), 231–238.

Melville, B. W. & Chiew, Y.-M. 1999 Time scale for local scour at bridge piers. *J. Hydraul. Engng* **125**(1), 59–65.

Melville, B. W. & Coleman, S. E. 2000 *Bridge Scour*. Water Resources Publications, Highlands Ranch, CO.

Mia, M. F. & Nago, H. 2003 Design method of time-dependent local scour at circular bridge pier. *J. Hydraul. Engng* **129**(6), 420–427.

Miller, M. C., McCave, I. N. & Komar, P. D. 1977 Threshold of sediment motion under unidirectional currents. *Sedimentology* **24**(4), 507–525.

Mueller, D. S. 1996 Local scour at bridge piers in nonuniform sediment under dynamic conditions. *Ph.D. Dissertation*. Colorado State University, Fort Collins, CO.

Mueller, D. S. & Wagner, C. R. 2005 Field observations and evaluations of streambed scour at bridges. *Report No. FHWA–RD–03–052*. U.S. Department of Transportation.

Muzzamil, M. & Ayyub, M. 2010 ANFIS-based approach for scour depth prediction at piers in non-uniform sediments. *J. Hydroinf.* **12**(3), 303–317.

Neill, C. R. 1973 *Guide to Bridge Hydraulics*. University of Toronto Press.

Oliveto, G. & Hager, W. H. 2002 Temporal evolution of clear-water pier and abutment scour. *J. Hydraul. Engng* **128**(9), 811–820.

Parola, A. C., Hagerty, D. G., Mueller, D. S., Melville, B. W., Parker, G. & Usher, J. S. 1997 The need of research on scour at bridge crossings. *Proc. 27th IAHR Congress*, International Association for Hydraulic Research, Delft, The Netherlands, pp. 124–129.

Rao, Z. & Alvarruiz, F. 2007 Use of an artificial neural network to capture the domain knowledge of a conventional hydraulic simulation model. *J. Hydroinf.* **9**(1), 15–24.

Richardson, E. V. & Davis, S. R. 1995 Evaluating scour at bridges. *Federal Highway Administration Hydraulic Engineering Circular No. 18, FHWA-IP-90-017* (3rd edn).

Sarle W. S. 1997 *Frequently asked questions on neural networks. IEEE Trans. on Neural Networks*, Cary, NC.

Shen, H. W., Schneider, V. R. & Karaki, S. 1969 Local scour around bridge piers. *J. Hydraul. Divis.* **95**(6), 1919–1940.

Sheppard, D. M. & Miller, W. Jr. 2006 Live-bed Local Pier Scour Experiments. *J. Hydraul. Engng* **132**(7), 635–642.

Sheppard, D. M., Odeh, M. & Glasser, T. 2004 Large-scale clear-water local pier scour experiments. *J. Hydraul. Engng* **130**(10), 957–963.

Solomatine, D. P. & Dulal, K. N. 2003 Model trees as an alternative to neural networks in rainfall–runoff modelling, *Hydrol. Sci. J.* **48**(3), 399–411.

Toth, E. 2009 Classification of hydro-meteorological conditions and multiple artificial neural networks for streamflow forecasting. *Hydrol. Earth Syst. Sci.* **13**, 1555–1566.

Tsanis, I. K., Coulibaly, P. & Daliakopoulos, I. N. 2008 Improving groundwater level forecasting with a feedforward neural network and linearly regressed projected precipitation. *J. Hydroinf.* **10**(4), 317–330.

Wang, W. C., Chau, K. W., Cheng, C. T. & Qiu, L. 2009 A comparison of performance of several artificial intelligence methods for forecasting monthly discharge time series. *J. Hydrol.* **374**(3–4), 294–306.